

Electrochemical characterization of supercapacitors based on carbons derived from coffee shells

M.R. Jisha^a, Yun Ju Hwang^a, Jae Sun Shin^c, Kee Suk Nahm^{b,*}, T. Prem Kumar^d, K. Karthikeyan^d, N. Dhanikaivelu^d, D. Kalpana^d, N.G. Renganathan^d, A. Manuel Stephan^d

^a Department of Hydrogen and Fuel cells Engineering, Chonbuk National University, Jeonju 561-756, Republic of Korea

^b Department of Hydrogen and Fuel cells Engineering, Chonbuk National University and School of Chemical Engineering and Technology, Jeonju 561-756, Republic of Korea

^c School of Nanosemiconductor display, Chonbuk National University, Jeonju 561-756, Republic of Korea

^d Central Electro Chemical Research Institute, Karaikudi 630006, India

ARTICLE INFO

Article history:

Received 28 April 2008

Received in revised form 2 October 2008

Accepted 5 November 2008

Keywords:

Supercapacitors

Carbon

Porogen

Coffee shells

Chemical activations

ABSTRACT

Carbons derived by pyrolysis of coffee shells treated with ZnCl_2 were used as electrode materials in symmetric electrochemical supercapacitors. Scanning electron microscopy showed that the carbon from the porogen-free shells show a flake-like structure, while those from the ZnCl_2 -treated coffee shells have a loose, disjointed structure with no definite shape. X-ray diffraction studies indicated the presence of small domains of coherent and parallel stacking of the graphene sheets. The average surface area of the carbon was $842 \text{ m}^2 \text{ g}^{-1}$, with an average micropore area of $400 \text{ m}^2 \text{ g}^{-1}$. Cyclic voltammetric studies suggested a specific capacitance of about 150 F g^{-1} . Self-discharge studies on the devices showed a large retention time.

© 2008 Elsevier B.V. All rights reserved.

1. Introduction

Electrochemical capacitors are attractive energy storage devices [1]. Energy storage in supercapacitors is achieved by faradaic and non-faradaic reactions at the electrode–electrolyte interface. As the reversibility of the double layer processes at the surface of an electroactive material determines the capacitor's performance, a high surface area is needed to achieve high capacitance. High surface area carbons are widely employed as electrodes for energy storage in double layer capacitors [2–10].

Supercapacitor stores the electric charge in the double layer formed at the electrode/electrolyte interface determined by the surface area and pore size distribution. For high-performance supercapacitor, both micropores (pore diameter $< 2 \text{ nm}$) providing a high surface area which play an essential role for charging the electrical double layer and determine the values of capacitance and mesopores ($2 \text{ nm} < \text{pore diameter} < 50 \text{ nm}$) allowing good electrolyte penetration providing high power density are required. Normally active carbons consist of micro–meso pores in wide ranges. These active carbons have been reported by many groups for supercapacitor applications [4–9]. Porous carbons with mesopores

sizes in a narrow range cannot be obtained with any known classical method for the preparation [10]. However, it is possible to achieve this by using inorganic templates or by pore-forming substances like ZnCl_2 . It is reported that microporous carbons can easily be synthesized by ZnCl_2 chemical activation at low impregnation ratios (mass of ZnCl_2 /raw material). Combinations of template and ZnCl_2 chemical activation were utilized to control the pore structure of the porous carbons. The pore size distribution changes from bimodal to unimodal after the addition of ZnCl_2 indicating the dispersion effect of ZnCl_2 on carbons [11–12].

Most of the research on carbon has been done with precursors which are either directly or indirectly related to the petroleum products or fossil fuels viz. graphite, etc. and hydrocarbons like methane, benzene, acetylene, butane, etc. For synthesizing novel carbon material as a viable product, it is necessary to select a precursor, which is not derived from fossil fuels or related to petroleum products. Hence, we opted 'Coffee Shells', a natural product, from which activated carbons can be synthesized by pyrolysis. Comparing with other carbon materials, activated carbons from coffee shells is one of the most promising materials for fabricating supercapacitors, because of its low cost, inherent surface area, structural stability and good electrochemical property in acidic aqueous electrolyte.

Hwang Yun Ju et al. reported production of disordered carbons by the pyrolysis of coffee shells and have shown higher capacities

* Corresponding author. Tel.: +82 63 270 2311 fax: +82 63 270 2306.

E-mail address: nahmks@chonbuk.ac.kr (K.S. Nahm).

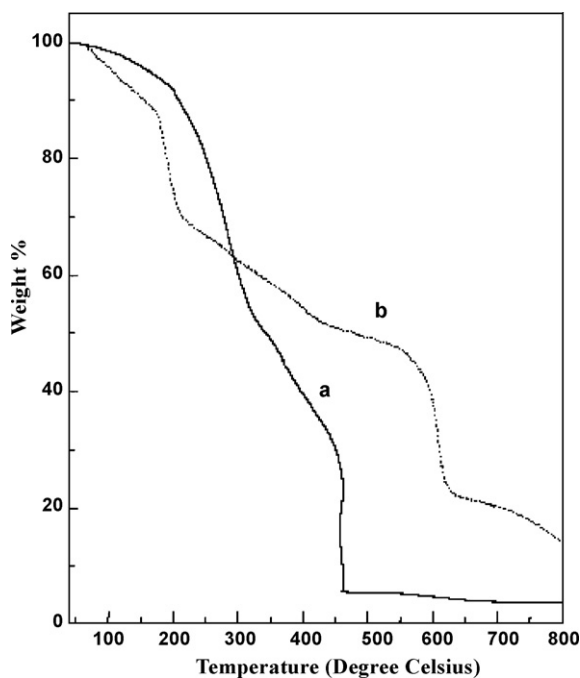


Fig. 1. TG traces of pre-cursor (a) coffee shells without porogen and (b) treated with ZnCl_2 (coffee shell: ZnCl_2 ratio = 1:10).

for lithium intake. The surface area of the carbon materials has been increased to 1.3 and 19.9 orders upon the addition of ZnCl_2 and KOH as porogen, respectively. The high capacities in these disordered carbons are attributed to the binding of lithium on extra surfaces of the single layers of carbon and in the nanocavities formed by the porogens.

The objective of this article is to prepare high-performance, low-cost carbon electrode materials from coffee shells and study the relation between the carbon property and performance of the supercapacitor. Though there are few literatures available on coffee shells carbon, to our knowledge, for the first time we have used carbon made from coffee shells have been used as electrode active material for supercapacitor applications. In this study, at first we tried to synthesize activated carbon of high surface area by using simple pyrolysis technique. The electrodes are characterized by cyclic voltammetry, impedance analysis, XRD, SEM and pore-size analysis.

2. Experimental

Dry, good quality coffee shells were purchased from the local sources (in India). The coffee shells were ground into a fine powder and then treated with concentrated solutions of ZnCl_2 (porogen) for 5 days at room temperature at coffee shell: porogen ratios of 1:5, 1:10, 1:20 by weight, and dried. They were then pyrolyzed at 900°C under nitrogen at a heating ramp of $10^\circ\text{C min}^{-1}$ and a hold period of 1 h. The pyrolytic carbons are designated in this paper as carbon (1:5), carbon (1:10) and carbon (1:20), respectively. Pyrolytic carbons were also obtained without ZnCl_2 treatment, in which case the coffee shells were simply heat-treated under the above conditions. This carbon is designated in this paper as porogen-free carbon. Powder X-ray diffraction patterns were recorded between 5° and 80° on X-ray diffractometer model (Rigaku D/Max 2500), fitted with a nickel-filtered $\text{Cu K}\alpha$ radiation source. The morphology of the pyrolytic carbons was examined by a Hitachi S-4700, field emission scanning electron microscope. BET (Brunauer, Emmett and Teller) surface area measurements were made by a Micromeritics ASAP2010 surface area analyzer.

2.1. Assembly of supercapacitors

Slurries of the carbon samples in *N*-methyl pyrrolidine were applied on nickel foam current collectors. The electrodes were kept in an oven at 250°C for 1 h and slowly cooled to room temperature. A polypropylene separator was sandwiched between the two carbon electrodes in a cell with 6M KOH as the electrolyte. The room temperature conductivity of the electrolyte was about $4 \times 10^{-2} \text{ S cm}^{-1}$. All the electrochemical measurements were carried in a two-electrode assembly consisting of carbon made from coffee shells. The geometrical area of the electrodes was 1 cm^2 .

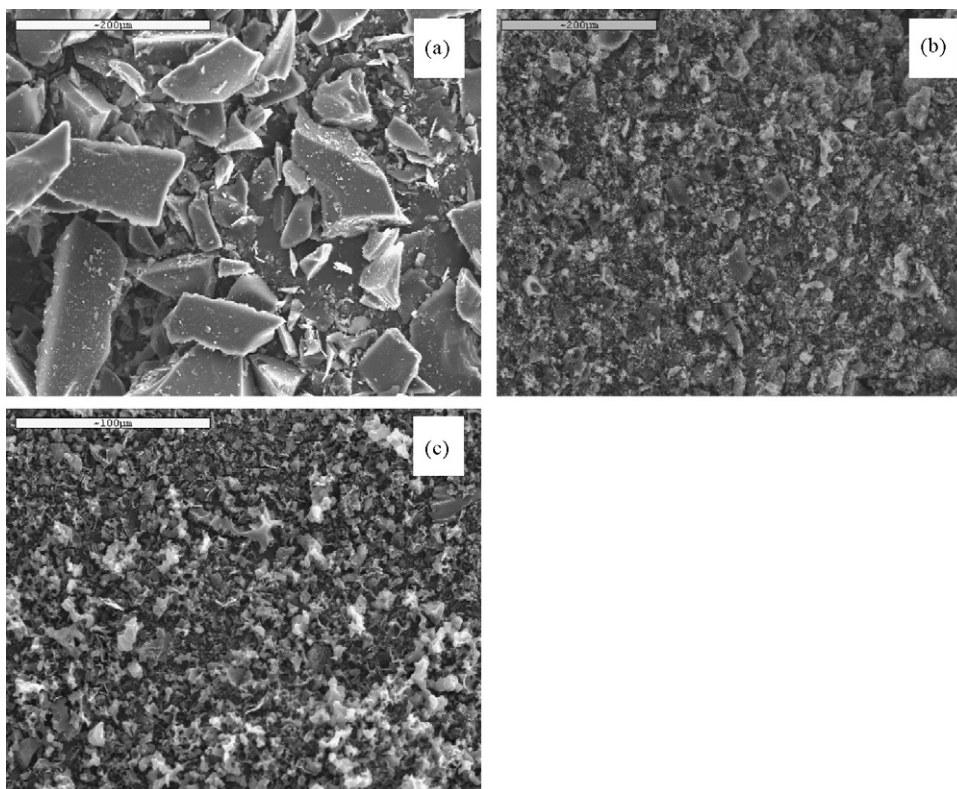


Fig. 2. SEM micrographs of carbon derived by pyrolysis of (a) untreated coffee shells; (b) carbon 1:10; and (c) carbon 1:20.

The cyclic voltammetric studies were run on a BAS 100 electrochemical analyzer. Impedance measurements of the cells were characterized by using PARSTAT 2263. The charge–discharge cycling properties of the cells were evaluated by using a Won-A Tech Battery cycler.

3. Results and discussion

3.1. Thermo gravimetric analysis

Fig. 1 depicts the thermograms of carbons obtained from untreated coffee shells and from coffee shells treated with ZnCl_2 (shell: ZnCl_2 = 1:10). The weight loss around 100°C is attributed to loss of superficial moisture from the shells. A major weight loss can be seen between 250 and 450°C , which can be attributed to the destructive distillation of the shells to yield low-volatile organics. The pyrolytic processes result in carbonization and attendant aromatic condensation. Slow organization of disoriented carbon layers is a continuous process that proceeds during the thermal treatment [13]. From the graph, the weight percentage represents the weight loss of both carbon and ZnCl_2 . The lower weight loss or the higher weight of the residual fraction is due to the presence of ZnCl_2 or by-products.

3.2. SEM and BET surface area

Fig. 2 depicts the SEM micrographs of pyrolytic carbons. The surface properties of the pyrolytic carbons were examined by a Hitachi S-4700, field emission scanning electron microscope. For preparing samples, the coffee shell carbons were mixed thoroughly with a spatula. To spread the activated carbon, a carbon tape was used as an adhesive base. The tape was pasted on the circular mount. Then the activated carbons were sprinkled on the tape and pressed lightly, and sprayed with canned air to remove any loose material from the top and then the samples were mounted on the SEM experimental set-up.

The carbons from the porogen-free shells show a flake-like structure, while those from the ZnCl_2 -treated coffee shells have a loose, disjointed structure with no definite shape. This peculiar morphology may be due to the escaping gases during the pyrolysis process [14]. The evolving gases generate pores in the carbon. During carbonization, ZnCl_2 acts as a dehydrating agent. Subsequent removal of unreacted ZnCl_2 by washing with water results in further pore generation [15].

The surface properties of pyrolyzed carbons play a vital role in the electrochemical properties of double layer capacitors. BET surface area measurements were made by a Micromeritics ASAP2010 surface area analyzer. Before measuring BET the activated carbons were dried and kept under 900°C and evacuated for 3 h. Nitro-

Table 1

The BET surface area, micropore area, Langmuir surface area, external surface area, micropore volume, single point adsorption total pore volume and pore size adsorption average pore diameter of 1:20 ZnCl_2 activated carbons and non-porogen carbons.

1:20 ZnCl_2 treated carbons	1:20 ZnCl_2 treated carbons	Non-porogen carbons
S_{BET} (BET surface area)	$842.4052 \text{ m}^2 \text{ g}^{-1}$	$37.2641 \text{ m}^2 \text{ g}^{-1}$
S_{micro} (micropore area)	$400.4386 \text{ m}^2 \text{ g}^{-1}$	$16.8705 \text{ m}^2 \text{ g}^{-1}$
Langmuir surface area	$1068.9712 \text{ m}^2 \text{ g}^{-1}$	$47.2023 \text{ m}^2 \text{ g}^{-1}$
S_{ext} (external surface area)	$441.9667 \text{ m}^2 \text{ g}^{-1}$	$20.3936 \text{ m}^2 \text{ g}^{-1}$
Micropore volume	$0.171486 \text{ cm}^3 \text{ g}^{-1}$	$0.007241 \text{ cm}^3 \text{ g}^{-1}$
Single point adsorption total pore volume	$0.466886 \text{ cm}^3 \text{ g}^{-1}$	$0.027606 \text{ cm}^3 \text{ g}^{-1}$
Pore size (adsorption average pore diameter)	22.1692 Å	29.6324 Å

gen was the analysis adsorptive during the measurement. The pore characteristics [16], viz., BET surface area, micropore volume, mesopore volume, total pore volume, mesoporosity, and mean pore diameter of the carbons are summarized in Table 1.

Typical nitrogen adsorption–desorption isotherms for carbon obtained from the untreated shells and for the carbon (1:20) are shown in Fig. 3a and b, respectively. The BET surface area for carbon (1:20) is $842.4 \text{ m}^2 \text{ g}^{-1}$ and that of the carbon from the untreated shells is $37.2 \text{ m}^2 \text{ g}^{-1}$. The hysteresis observed in the isotherms is attributed to the mesoporosity of the materials [17].

3.3. X-ray diffraction

XRD patterns of the porogen-free carbon and the carbons obtained from ZnCl_2 treated shells are shown in Fig. 4. Powder X-ray diffraction patterns were recorded on X-ray diffractometer model (Rigaku D/Max 2500), fitted with a nickel-filtered $\text{Cu K}\alpha$ radiation source. The specimens were prepared by spreading coffee shells carbon on an adhesive tape on a glass slide. After smoothening the surface, it was made uniform through out. Then the specimen was mounted on the mount of the diffractometer and the start angle and stop angle were set to be 5° and 80° , respectively (at 40 kV and 30 mA). The reflections around 43° corresponds to the (100) plane and indicate the presence of honeycomb structures formed by sp^2 hybridized carbons. The broad reflections of (002) between 20° and 30° indicate small domains of coherent and parallel stacking of graphene sheets. As indicated by Liu et al. [18], the quantity of single layers in carbon materials pyrolyzed at low temperatures can be estimated from the empirical “R” factor. Generally, the value of the “R” factor is an estimate of the fraction of non-parallel single layers of carbon. In the present study, the value of R is more than 2 for all the carbons. The increase in “R” factor value of

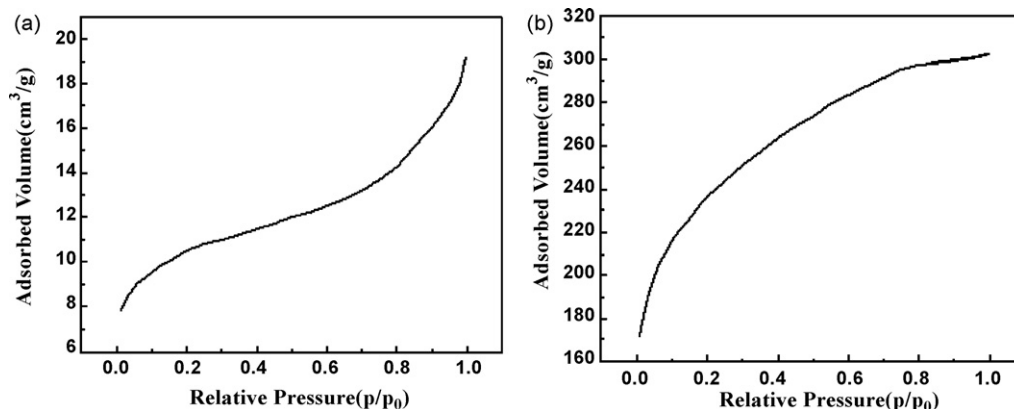


Fig. 3. BET isotherm of pyrolytic carbons. (a) Derived from untreated coffee shells (BET surface area: $37 \text{ m}^2 \text{ g}^{-1}$) and (b) carbon (1:20) (BET surface area: $842 \text{ m}^2 \text{ g}^{-1}$).

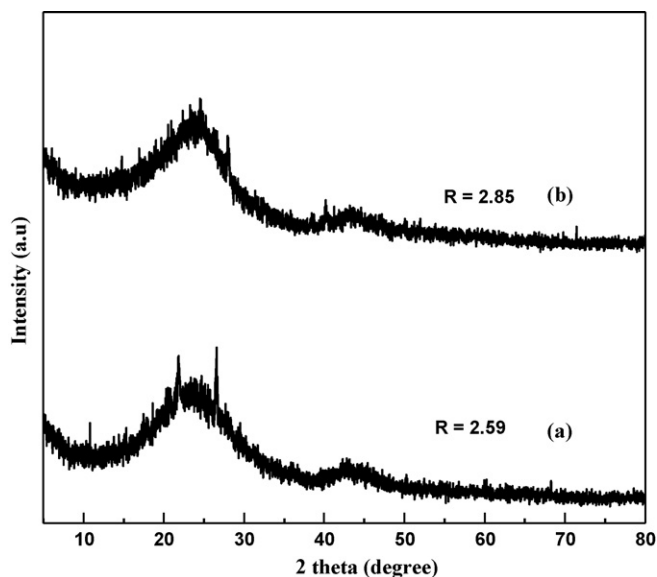


Fig. 4. X-ray diffractogram of pyrolytic carbon; (a) untreated and (b) carbon (1:20).

the carbon due to ZnCl_2 treatment suggest exothermic processes in the treated shells during which single layers become mobile resulting in increased ordering of the layers. Prolonged and/or high-temperature processing can lead to single carbon layers aligning themselves into small domains of ordered structures, eventually tending towards graphitic structures [19]. As discussed by Fey et al. [20], the porogens do not alter the crystallographic parameters of the products. However, an increase in the d_{002} values has been observed for carbons derived from the porogen-treated coffee

shells. This is attributed to the disoriented nature of the single layers, which can lead to increased spacings between adjacent carbon layers.

As a measure of number of carbon sheets one can use the empirical parameter, R , defined by the ratio of the 002 Bragg angle peak to the background [21]. In the present study, we use the simple definition for quick and easy comparison of the samples obtained from the precursors heated at different temperatures.

4. Electrochemical characterizations

4.1. Cyclic voltammetry

Cyclic voltammograms of carbons 1:5, 1:10 and 1:20 and non-porogen carbons (and this will be referred in our discussion throughout the paper) at different scan rates are shown in Fig. 5a–d, respectively. The influence of the scan rate on the specific capacitance is evident from the figures, and it is seen that an increase in the non-faradaic current is observed with an increase in the scan rate. For all the carbons, cyclic voltammograms are rectangular and only at higher scan rates, a prolate rectangle is observed. This implies that the carbons obtained from the coffee shells have good capacitor performance. The prolate rectangle may be due to diffusion-limited capacitance, which may in turn be due to electrolyte trapped in the micropores of the carbons [22–23]. It is clear that (1:20) is better, compared to (1:10) and (1:5) at all scan rates. It is well known that for porous carbons, higher the capacitance, longer is the time required to acquire/release charges. Cyclic voltammogram of non-porogen carbons show prolate rectangular shape at a sweep rate of 10 mV and it gives a capacitance of 15 Fg^{-1} . The reason of the low capacitative property may be due to the less number of micropores in the non-porogen carbons. As the micropores are less there is a lowering in the diffusion-limited capacitance, which is caused by

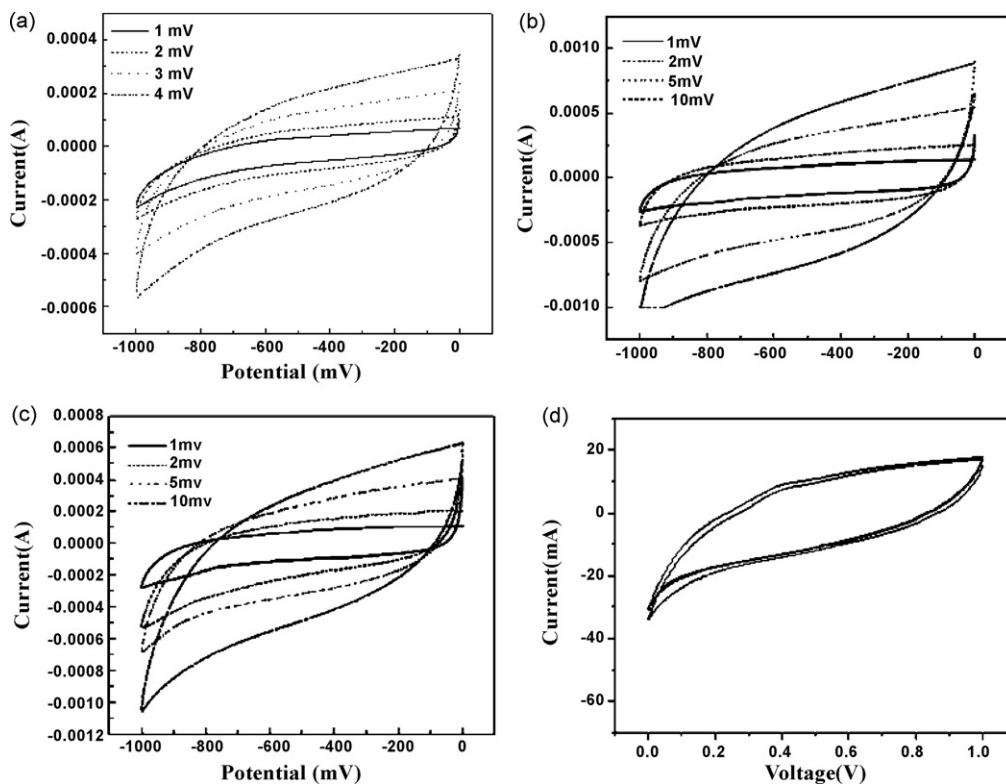


Fig. 5. Cyclic voltammograms of carbons derived by the pyrolysis of ZnCl_2 -activated coffee shells with shell: ZnCl_2 ratios of (a) 1:5; (b) 1:10 and (c) 1:20 at different sweep rates and (d) non-porogen carbons at sweep rate 10 mV.

Table 2
The specific capacitance of the carbons calculated from cyclic voltammetry measurements.

Scan rate	Specific capacitance for carbon (1:5)	Specific capacitance for carbon (1:10)	Specific capacitance for carbon (1:20)	Specific capacitance for non-porogen carbon
1 mV s ⁻¹	40.1 F g ⁻¹	77.6 F g ⁻¹	156 F g ⁻¹	–
2 mV s ⁻¹	34.7 F g ⁻¹	26.4 F g ⁻¹	138 F g ⁻¹	–
5 mV s ⁻¹	24.4 F g ⁻¹	36.2 F g ⁻¹	77 F g ⁻¹	–
10 mV s ⁻¹	17.3 F g ⁻¹	38.3 F g ⁻¹	50 F g ⁻¹	15 F g ⁻¹

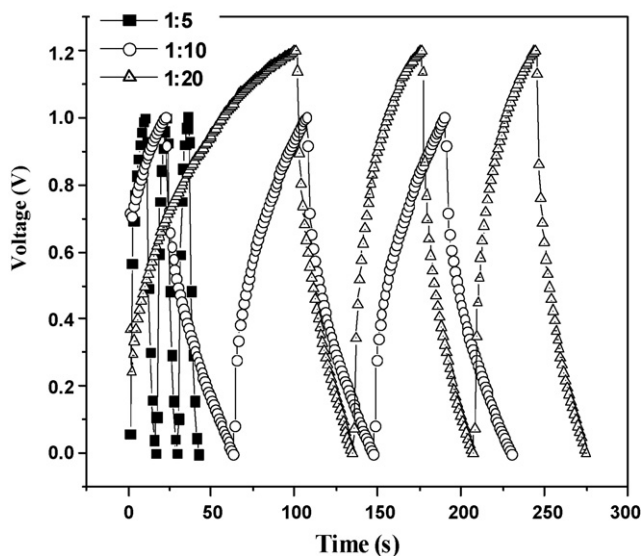


Fig. 6. Charge–discharge behavior of carbons derived by pyrolysis of coffee shells treated with different amounts of ZnCl₂.

the electrolyte tapped in the micropores of the carbons. In addition to this, the performance of the untreated carbon materials is studied by Li et al. [23].

However, the capacitance obtained may not be commensurate with the surface area and this may be caused by the capacitance of mesoporous area [7–12]. The increased microporosity is due to the dispersion effect of ZnCl₂, and the pore size distribution could have been changed from bimodal to unimodal upon the addition of ZnCl₂. The specific capacitance of the carbons derived from the porogen-treated coffee shells, as calculated from cyclic voltammetric measurements, are presented in Table 2. It is clear that the specific capacitance for the carbon (1:20) ratio is higher at all the scan rates studied. From Table 2, it can be seen that the EDLC performance drops drastically when the CV scan rate is increased from 1 to 10 mV for all the carbons studied. The high specific capacitance is observed at the lowest scan rate (1 mV s⁻¹). It may be due to that, the ions can transport into pores more easily at the low scan rate. However, ions cannot diffuse into the pores when each fast cycle is completed. The mechanism of electrochemical storage between activated carbon electrodes could be described by the electrical double layer theory and it is suggested that ions can occupy some pores within the electrode to participate in the formation of the electrochemical double layer. So at higher scan rates when each cycle finishes very faster, the ions cannot diffuse in to the pores as

faster as the cycles are completed. This could be the reason for such a poor performance at the higher scan rates.

4.2. Charge–discharge studies

The charge–discharge patterns of carbons 1:5, 1:10 and 1:20 at the voltage range of 0–1.2 V are displayed in Fig. 6. It is seen that carbon 1:20 discharges over a long time and that its capacitance is the highest among the carbons studied here. A capacitance value of 150 F g⁻¹ could be realized with this carbon. What is remarkable is that such a high capacitance could be obtained without the use of ruthenium oxide additives. The electrodes have a stable electrochemical property in 6 M KOH electrolyte with different currents. Pore size distribution is one of the key factors that dictate the selection of activated carbon materials for EDLCs. From Table 1, the BET surface area of the 1:20 carbons is 842.4052 m² g⁻¹ which is very large pore area. From Table 2, the specific capacitance of the 1:20 carbons is 156 F g⁻¹. So as the cut off voltage is increased the diffusion of the ions into the carbon is more. It is very significant in terms of capacitance that the surface areas of the 1:20 carbons are more. Because of the increase in cut off voltage and the increase in the surface area the capacity is more for 1:20 carbons. As the upper cut off voltage is high, it will significantly increase the diffusion of ions at the electrodes, which has numerous numbers of pores in it.

Thus, the carbons synthesized from coffee shells treated with ZnCl₂ as a porogen will be highly suitable for supercapacitor applications. Table 3 compares specific capacitance and surface area of carbon 1:20 with those of activated carbons and carbon aerogel. It is seen that carbon 1:20 fares well from the specific capacitance and from the cycle life points of view [23–24].

‘Charging and discharging voltage’ as a function of time (constant current measurement, CC) and specific capacitance as a function of voltage (cyclic voltammetry measurement, CV) are routine supercapacitor test methods. In CC measurements, the test cell is subjected to a cyclic square-wave current, and the voltage response is measured as a function of time, which commonly shows the saw-tooth-like shape. In CV measurements, voltage sweep with saw-tooth shape wave is applied to the test cell, and the current response is recorded, which is typically a rectangular or parallelogram shape. So we have chosen a voltage window of –1 to 0. In this present study, for charge–discharge measurement, the voltage limits were set between 0 and 1.2 V to avoid the decomposition of aqueous electrolyte. Here we have used 6 M KOH which would not be decomposed in a voltage range of 0 to 1.2 V. As the parameters (time and voltage), with respect to which, the cyclic voltammetry and charge–discharge are measured, are different, there are two different voltage windows for the supercapacitor test cell for the CC and CV.

Table 3
Comparison of double layer capacitance, surface area and specific capacitance of activated carbons, carbon aerogel and ZnCl₂ activated carbons.

	Electrolyte	DC (μF cm ⁻²)	Surface area (m ² g ⁻¹)	Specific capacitance (F g ⁻¹)
1. Activated carbon	10% NaCl	19	1200	228 [24]
2. Carbon aerogel	4 M KOH	23	650	150
3. Carbon 1:20	6 M EOH	18.5	842	156 [present work]

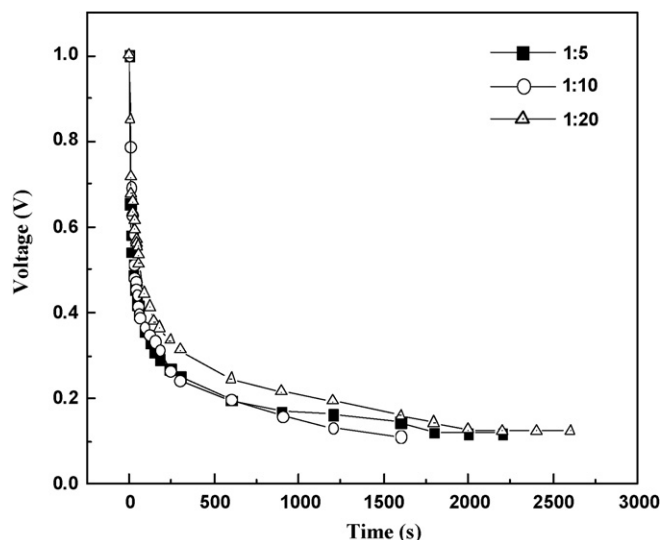


Fig. 7. Self-discharge curves for the various carbons.

4.3. Self-discharge

Self-discharge is a common phenomenon in charge storage devices such as batteries and electrochemical capacitors. It is defined as the rate of decline of the voltage of electrochemical power source with time on open-circuit following charging. The self-discharge behavior of the electrodes with carbons 1:5, 1:10 and 1:20 are shown in Fig. 7.

It is clear that from the self-discharge point of view that carbon with 1:20 is a good candidate for supercapacitor applications. Obviously, the large number of pores as well as their structure generated by ZnCl_2 during the formation of carbon 1:20 play a decisive role in ion transport and charge retention.

4.4. Analysis of impedance measurements

Electrochemical impedance studies on the carbon electrodes are shown in Fig. 8. A small semicircle corresponding to double layer

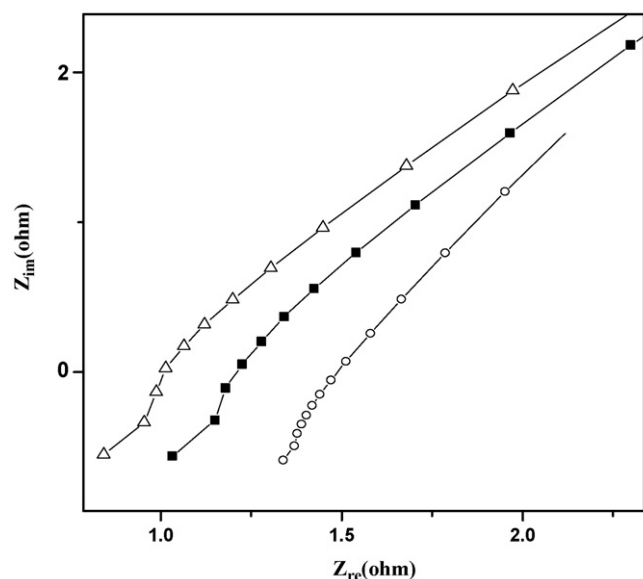


Fig. 8. Nyquist plots for the various carbon samples.

Table 4

Impedance parameter for carbons with different ratios of ZnCl_2 , i.e. 1:5, 1:10 and 1:20.

	R_s (Ω)	R_{ct} (Ω)	C_{dl} (mF g^{-1})
Ruthenium with weight percentage equal to 9	2	65	62.83
Carbons derived by the pyrolysis of ZnCl_2 , activated coffee shells with the ratio 1:20	1.179	0.01	5.073

charging, the charge transfer resistance and diffusion-controlled Warburg parts are seen in the plots. The knee frequency, the frequency at which there is a deviation from the semicircle for our samples, occurs much earlier in terms of both imaginary and real impedance components as compared to that of a composite electrode reported in [13]. This indicates that the carbons prepared from coffee shells are good capacitor material for supercapacitor applications. Various parameters such as the solution resistance (R_s , Ω), charge transfer resistance (R_{ct} , Ω) and double layer capacitance (C_{dl} , derived on the basis of the Randles equivalent circuit are given in Table 4.

A comparison of these values with coconut shell-ruthenium composite electrode [13] is also given. R_s is less (1.2Ω) compared to 2Ω for a composite electrode with 9 wt.% Ru. The value of R_{ct} is much lower ($1 \times 10^{-2} \Omega$) compared to that of composite electrode (65Ω).

Figs. 9 and 10 show the evolution of $C(\omega)$ normalized by $C(1 \text{ mHz})$ vs. frequency. These plots provide a convenient method to show the frequency response of supercapacitors because frequency is a dependant variable, unlike in the Nyquist plots where frequency is buried in both the real and imaginary impedance terms. Fig. 9 indicates a transition between purely resistive behavior, where $C(\omega)/C(1 \text{ mHz})$ is equal to zero ($R^2 C^2 \omega^2 \gg 1$) to purely capacitive behavior. Ideally, for capacitor applications the capacitance should remain nearly invariant with frequency, once this transition $R^2 C^2 \omega^2 \sim 1$ is passed [21]. Fig. 10 indicates the cutting of tangent at three different points for the three carbons. Transition occurs at these points which are characteristic of the entire system. The reciprocal of the characteristic frequency yields the time constant τ , which is a quantitative measure of how fast the device can be charged and discharged reversibly.

It is apparent that the characteristic time constants of the carbons increased with the amount of porogens in the precursor (Fig. 11). The increase in time constant is greater than that of ESR

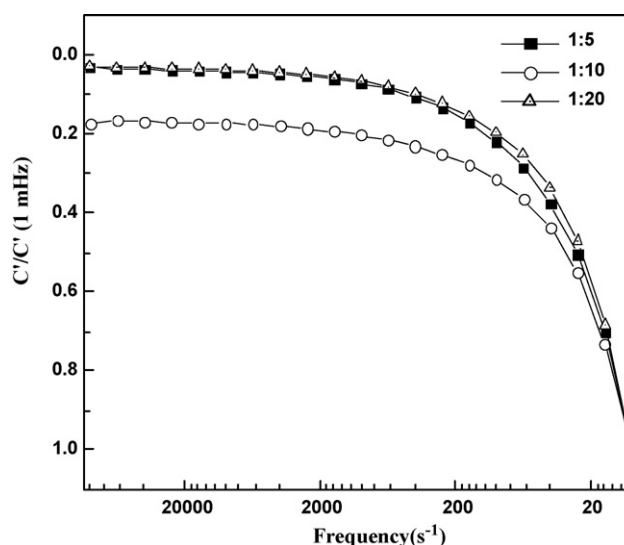


Fig. 9. Normalized real capacitance of the various pyrolytic carbons.

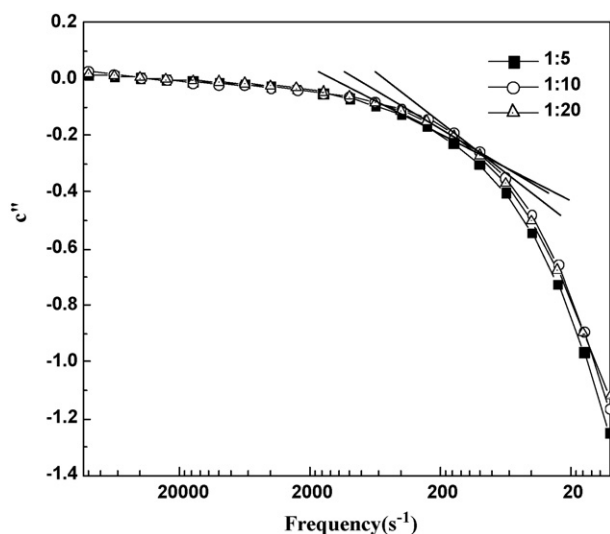


Fig. 10. Normalized imaginary capacitance vs. frequency for the pyrolytic carbons.

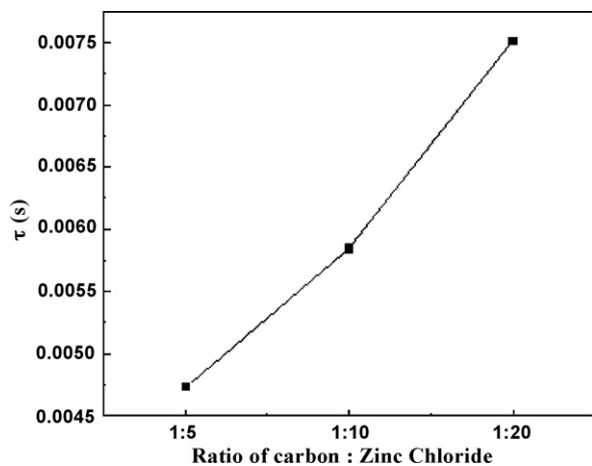


Fig. 11. A plot of time constant as a function of the shell:ZnCl₂ ratio in the precursor.

and it can be easily understood that the Langmuir surface area of the pore has a positive effect on the time constant.

5. Conclusions

Activated carbons were obtained from coffee shells treated with ZnCl₂. Nitrogen adsorption analysis revealed an average BET sur-

face area of 842 m² g⁻¹ and a micropore area of 400 m² g⁻¹ which suggest that these carbons have a predominance of macropores. A capacitance of around 150 F g⁻¹ was obtained for a symmetric supercapacitor assembled with these carbons. Charge transfer resistance was low compared to the carbons obtained from coconut shell composite electrode with ruthenium oxide. The limiting capacitance obtained was 0.185 F m⁻². Hence, the carbons obtained from the present method have enormous capacitive properties and is highly suitable for supercapacitor applications.

Acknowledgements

This work was supported by the Korean Research Foundation and Korean Federation of Science and Technology Societies Grant funded by the Korea Government (MOEHRD, Basic Research Promotion Fund). We would like to thank Korea Basic Science Institute, Korea (Jeonju branch) for use of their BET facility.

References

- [1] B.E. Conway, *Electrochemical Supercapacitors—Scientific Fundamentals and Technological Applications*, Kluwer Academic Publisher, Plenum Press, Dordrecht, NY, USA, 1999, pp. 183–220.
- [2] C. Niu, E.K. Sichel, D. Mry, H. Tennent, *Appl. Phys.* 70 (1997) 1480–1482.
- [3] D. Qu, H. Shi, *J. Power Sources* 74 (1998) 99–107.
- [4] H. Shi, *Electrochim. Acta* 41 (1996) 1633–1639.
- [5] R. Kotz, M. Carlen, *Electrochim. Acta* 45 (2000) 2483–2498.
- [6] M. Endo, T. Takeda, Y.J. Kim, K. Koshiba, K. Ishii, *Carbon Sci.* 1 (2001) 117–128.
- [7] E. Frackowiak, F. Beguin, *Carbon* 39 (2001) 937–950.
- [8] B.K.H. An, W.S. Kim, Y.S. Park, Y.C. Choi, S.M. Lee, D.C. Chung, *Adv. Mater.* 13 (2001) 497–500.
- [9] Ch. Emmanegger, Ph. Mauron, P. Sudan, P. Wenger, V. Hermann, R. Gally, *J. Power Sources* 124 (2003) 321–329.
- [10] T. Kyotani, *Carbon* 38 (2000) 269–286.
- [11] J. Lee, S. Yoon, S. Oh, C. Shin, T. Hyeon, *Adv. Mater.* 12 (2000) 359–362.
- [12] H. Zhou, S. Zhu, M. Hibino, I. Honma, *J. Power Sources* 122 (2003) 219–223.
- [13] M.S. Dandekar, G. Arabale, K. Vijayamohan, *J. Power Sources* 141 (2005) 198–203.
- [14] Y.J. Hwang, S.K. Jeong, K.S. Nahm, A.M. Stephan, *J. Alloys. Compd.* 448 (2007) 141.
- [15] Y.J. Hwang, S.K. Jeong, K.S. Nahm, J.S. Shin, A.M. Stephan, *J. Phys. Chem. Solids* 68 (2007) 182–188.
- [16] A. Janes, H. Kurig, E. Lust, *Carbon* 45 (2007) 1226–1233.
- [17] J. Zhao, C. Lai, Y. Dai, J. Xie, *Mater. Lett.* 61 (2007) 4639–4642.
- [18] Y. Liu, J.S. Xue, J.R. Dahn, *Carbon* 34 (1996) 193–200.
- [19] A.M. Stephan, T. Prem Kumar, R. Ramesh, S.K. Sabu Thomas, K.S. Jeong, Nahm, *Mater. Sci. Eng. A* 430 (2006) 132–137.
- [20] G.T.K. Fey, D.C. Lee, Y.Y. Lin, T. Prem Kumar, *Synth. Met.* 139 (2003) 71–80.
- [21] Y. Liu, J.S. Xue, T. Zheng, J.R. Dahn, *Carbon* 34 (1996) 193–200.
- [22] J. Chimola, G. Yushin, R. Dash, Y. Gogotsi, *J. Power Sources* 158 (2006) 765–772.
- [23] J. Li, X. Wang, Q. Huanga, S. Gamboab, P.J. Sebastian, *J. Power Sources* 158 (2006) 784–788.
- [24] C. Zhou, T. Liu, T. Wang, S. Kumar, *Polymer* 47 (2006) 5831–5837.